A novel method to rapidly functionalize perovskite oxide

Weiwei Fan*[,1], Zhu Sun*[,2], Rui Xiao[1]

[1]Key Laboratory of Energy Thermal Conversion and Control of Ministry of Education, School of Energy and Environment, Southeast University, 2 Dong Nan Da Xue Road, Nanjing, 211189, China

[2]School of Materials Science and Engineering, Shanghai Jiao Tong University, 800 Dongchuan Road, Shanghai, 200240, China

*Corresponding author email: fanww@seu.edu.cn

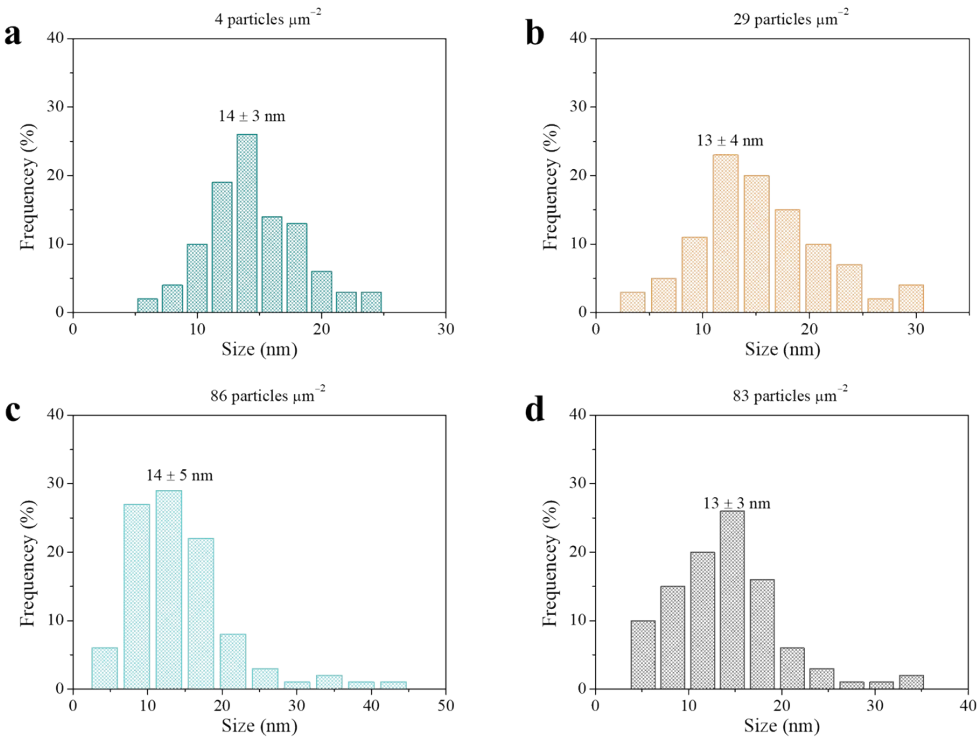

Figure S1 Particle size distribution of (a) PN3, (b) PN6, (c) PN9 and (d) PN12 after P-V shock.

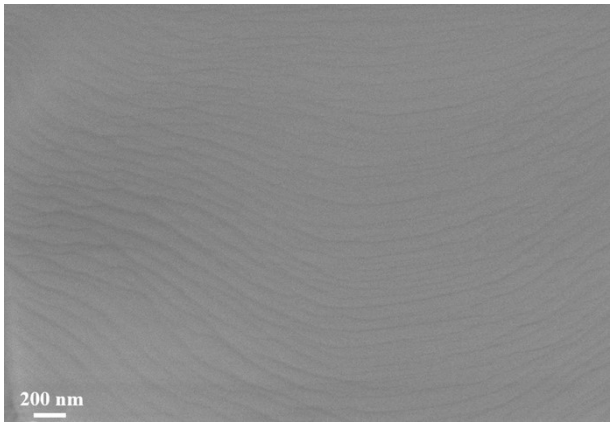

Figure S2 SEM image of the LCTN treated by voltage shock.

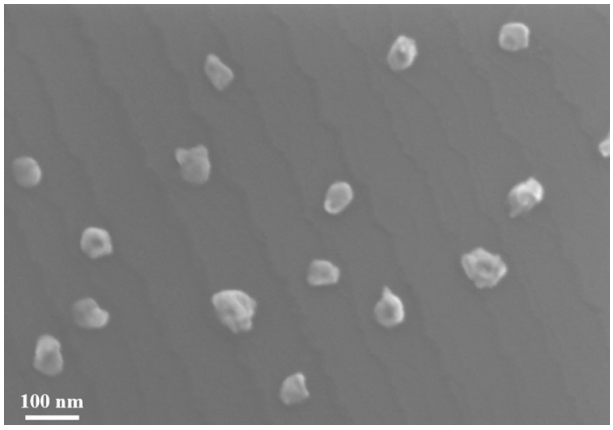

Figure S3 SEM image of LCTN treated in H_2 at 900℃ for 20h.

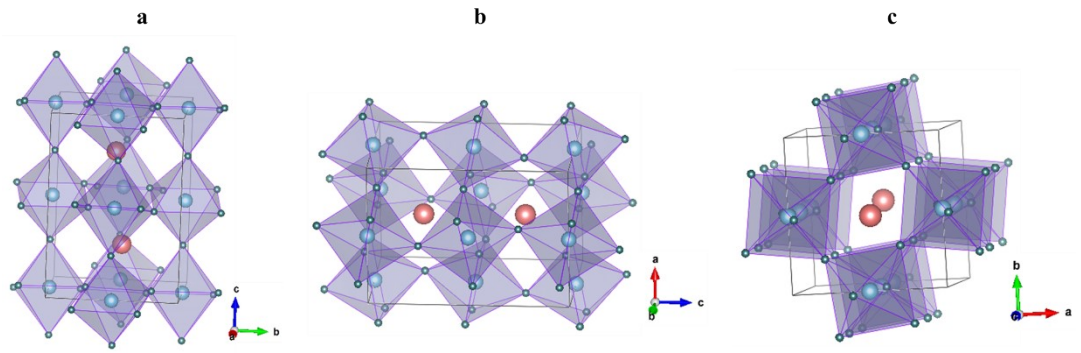

Figure S4 a-c, Views of orthorhombic structure of LCFN perovskite. Pink spheres denote La/Ca, blue spheres denote Ti/Ni, and green spheres denote O, respectively.

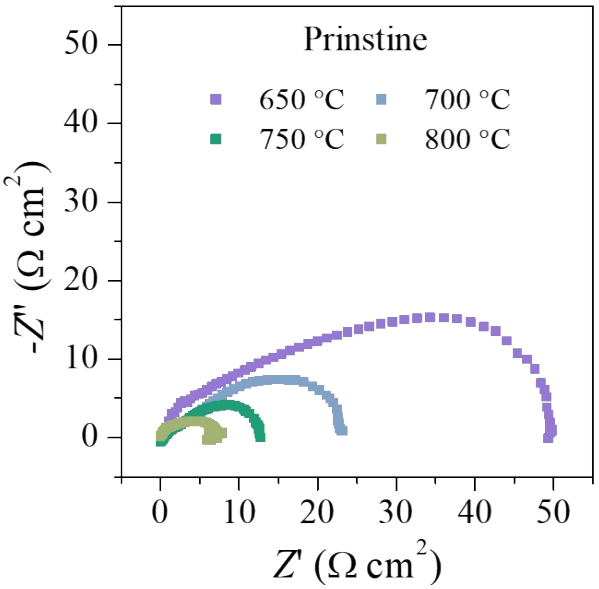

Figure S5 Nyquist plots of the pristine LCTN under OCV.

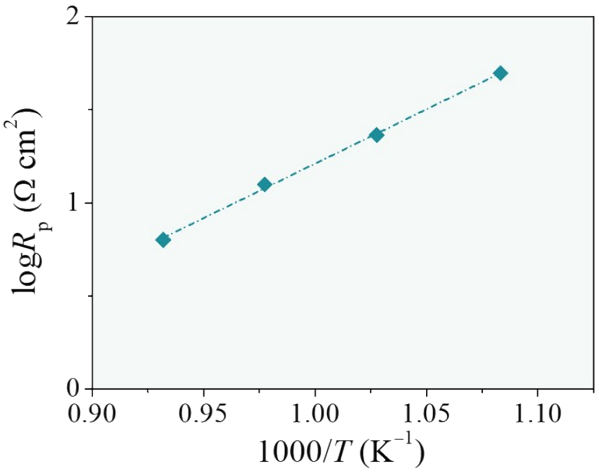

Figure S6 Arrhenius plot of R_p of the pristine LCTN.

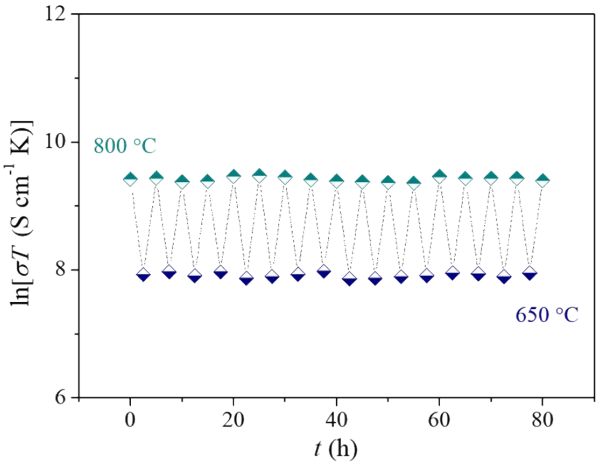

Figure S7 Thermal cycling stability of LCTN-PN9 in hydrogen.

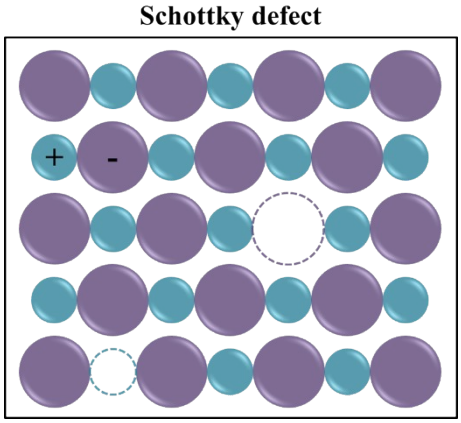

Figure S8 Illustration of Schottky defect in perovskite solid.

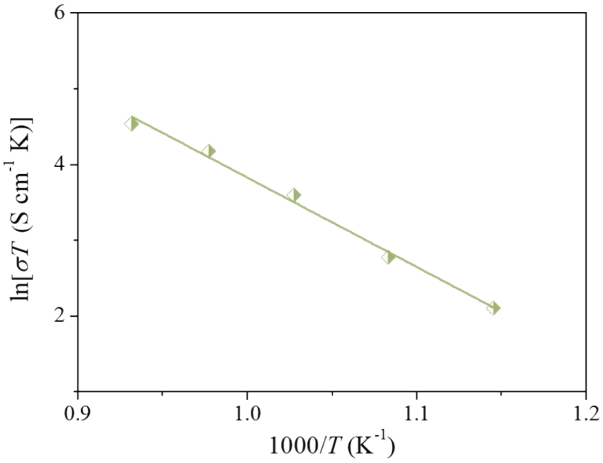

Figure S9 Electrical conductivity of pristine LCTN at different temperatures in hydrogen.

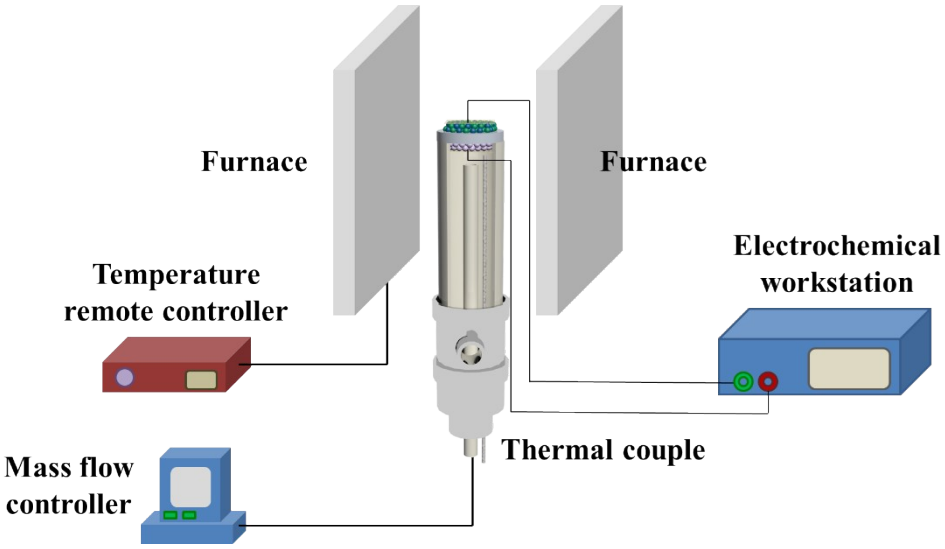

Figure S10 Schematic of the home-made setup used for the cell performance tests.

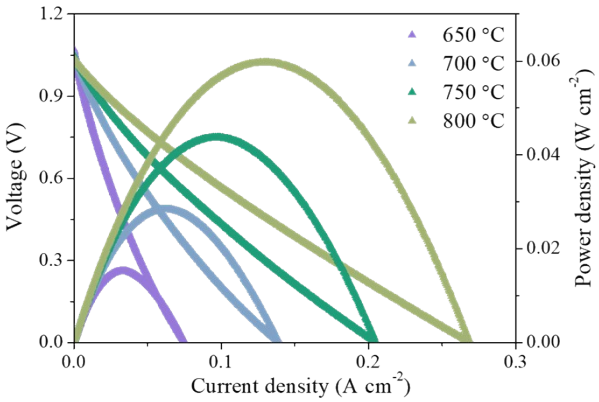

Figure S11 *I-V*(*P*) curves of the pristine LCTN collected at different temperatures.

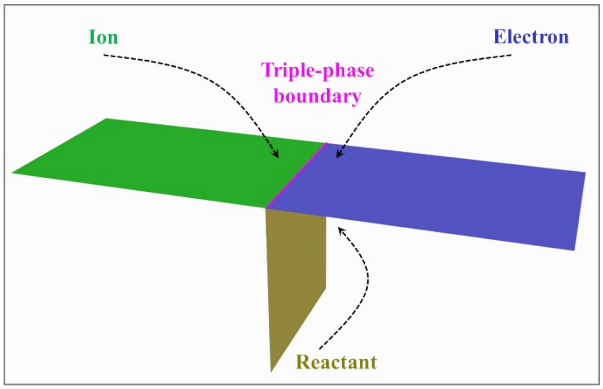

Figure S12 Schematic illustration of the triple-phase boundary.

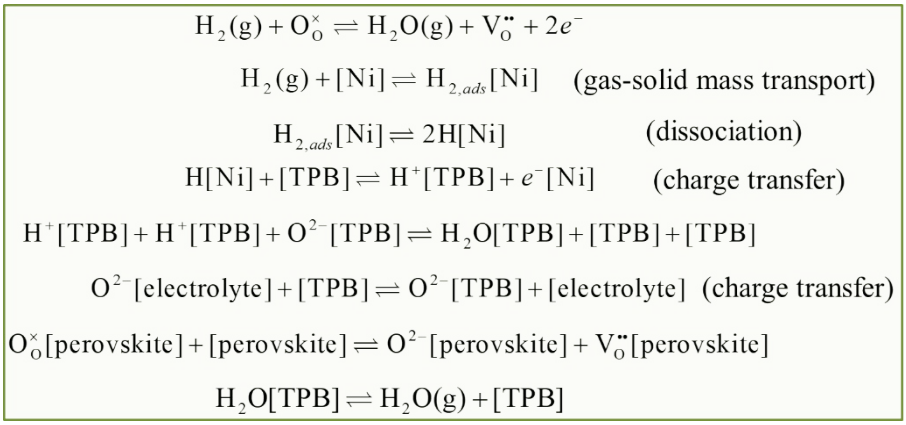

Figure S13 Procedures for the electrochemical oxidation of hydrogen under the assistance of exsolved nickel nanoparticles. Note: in the expressions, H[Ni] represents the atomic hydrogen adsorbed on Ni, [Ni] represents a vacant site on the surface of Ni, e^- repents an electron in Ni and $O_O^{\times}$ represents lattice oxygen, respectively.

Note 1:

Exsolution depth

Assuming the exsolved particle is a sphere, then the volume of a particle can be calculated by

$$V = \frac{4}{3}\pi(\frac{D}{2})^3$$

where D is the diameter of particle. In a particle, the number of metal atoms is evaluated by

$$N = \frac{\rho V}{A_M \times 1.661 \times 10^{-27}}$$

where ρ represents the mass density of metal (ρ_{Ni} = 8900 kg m^{-3}), A_M represents the atomic mass of metal (A_{Ni} = 58.69). Then, the number of metal atoms (Ni) exsolved from per surface area (N_{SA}) can be acquired as follows

$$N_{SA} = N \times P_D$$

where P_D is the particle density obtained experimentally. Then, the number of exsolvable metal atoms per surface area and per depth in nanometer (N_V) can be calculated from

$$N_V = \frac{0.06}{0.54623 \times 0.77317 \times 0.54623} = 0.26\text{nm}^{-3}$$

where 0.06 is the atomic ratio of Ni in a unit cell, and 0.54723 nm × 0.77275 nm × 0.54698 nm is the unit cell parameters obtained from the Rietveld refinement of XRD. Then, the depth (D_{ep}) can be evaluated from

$$D_{ep} = \frac{N_{SA}}{N_V}$$

Table S1 Chemical composition of the as-prepared LCTN measured by ICP-AES.

Sample	La:Ca:Ti:Ni atomic ratio	
	Designed	ICP
$La_{0.32}Ca_{0.48}Ti_{0.94}Ni_{0.06}O_3$	0.32:0.48:0.94:0.06	0.323:0.482:0.938:0.058

Table S2 Refined structural parameters of LCTN obtained by fitting of the powder XRD data at room temperature.

Atoms, sites	Parameters	LCTFN
	Space group	Pbnm (62)
	a (Å)	5.4723 (3)
	b (Å)	7.7275 (2)
	c (Å)	5.4698 (3)
	V (Å^3)	231.3
La, 4c	x	0.4670
	y	0.2500
	z	0.0072
	Occupancy	0.32
Ca, 4c	x	0.4670
	y	0.2500
	z	0.0072
	Occupancy	0.48
Ti, 4a	x	0
	y	0
	z	0
	Occupancy	0.94
Ni, 4a	x	0
	y	0
	z	0
	Occupancy	0.06
O1, 4c	x	0.5107
	y	0.2500
	z	0.5722
	Occupancy	1
O1, 8d	x	0.2158
	y	0.0346
	z	0.2826
	Occupancy	1
	R_{wp}	11.31
	R_p	8.10
	χ^2	6.23

Table S3 Thermodynamic parameters of reducing the corresponding oxide to metal at 800 ℃

Metal oxides	ΔH (kJ mol^{-1})	ΔS (J K^{-1} mol^{-1})	ΔG (kJ mol^{-1})	Equilibrium constant K
La_2O_3	1038.132	106.908	923.404	1.123E-45
CaO	387.012	49.378	334.023	5.500E-17
TiO_2	442.309	65.134	372.410	7.443E-19
NiO	-13.012	31.182	-46.474	1.829E+02